

### Polarization of Gamma-Radiation Following Capture of Polarized Neutrons\*

L. C. BIEDENHARN, M. E. ROSE, AND G. B. ARFKEN  
Oak Ridge National Laboratory, Oak Ridge, Tennessee  
(Received June 14, 1951)

IN an attempt to utilize polarized neutrons for purposes of nuclear spectroscopy we were led to a consideration of the anisotropy properties of the emitted gamma-rays.<sup>1</sup> It is well known that for the capture of *s*-neutrons the intensity is isotropic. Therefore, the question arises of obtaining information concerning angular momentum of compound states and/or multipolarity of the  $\gamma$ 's by looking for anisotropy with polarization-sensitive detectors.

It can be shown that with ordinary Compton scattering, pair formation, or photoelectric processes as detection devices (all of which measure linear polarization) no anisotropy will occur. The probability that a neutron with polarization  $\mathbf{P}_0$  will lead to the emission of a photon with propagation vector  $\mathbf{k}$  and polarization vector  $\mathbf{e}$  is

$$W(\mathbf{P}_0, \mathbf{k}, \mathbf{e}) \sim \sum_{m_0 m'} | \sum_m (A(\mathbf{P}_0, m_0) | H_c | B_m) (B_m | H_2(\mathbf{k}, \mathbf{e}) | C_{m'})^* |^2 \quad (1)$$

with  $A$ ,  $B$ , and  $C$  representing probability amplitudes of initial, intermediate, and final states, respectively;  $m_0$ ,  $m$ , and  $m'$  the magnetic quantum numbers of target, compound, and final nuclear states. The angular momenta of these states are  $J_0$ ,  $J$ , and  $J'$ , respectively.  $H_c$  and  $H_2 \sim \alpha \cdot \mathbf{A}$  are the capture and  $\gamma$ -emission interaction operators; for the emission of plane polarized radiation the vector potential  $\mathbf{A}$  is

$$\mathbf{A}(\mathbf{k}, \mathbf{e}) = \sum_{P=\pm 1} e^{-iP\tau} \mathbf{A}(\mathbf{k}, P), \quad (2)$$

where  $\mathbf{e}$  makes an angle  $\tau$  with respect to a fixed direction in the plane normal to  $\mathbf{k}$  and  $\mathbf{A}(\mathbf{k}, P)$  corresponds to right ( $P=1$ ) and left ( $P=-1$ ) circularly polarized radiation.<sup>2</sup> The result for the intensity, in the linearly polarized case, for emission of a general multipole mixture is

$$W(\mathbf{P}_0, \mathbf{k}, \mathbf{e}) \sim \sum_L [(2J'+1)/(2L+1)] |a(JJ'L)|^2 \pm \frac{2|P_0|}{2J_0+1} \sin 2\tau \sum_{L < L'} \sum_M \text{Im} [a(JJ'L)a^*(JJ'L')] \times \sum_P P^{L-L'+1} D_{MP}^{(L)}(0\theta 0) D_{M, -P}^{(L')}(0\theta 0) \times \sum_{m m'} C_{J m M}^{J L C} C_{J m M}^{J L' C} \quad (3)$$

where the polarization-dependent part arises from the interference between different multipoles (order  $2L$  and  $2L'$ ). In (3) the  $\pm$  corresponds to  $J=J_0 \pm \frac{1}{2}$ , the  $a$  coefficients are reduced matrix elements<sup>3</sup> (independent of magnetic quantum numbers but dependent on parity), the  $D^{(L)}$  factors are the rotation matrices of order  $L$ ,  $\theta$  is the angle between  $\mathbf{k}$  and  $\mathbf{P}_0$ , and the  $C$ 's are vector addition coefficients.<sup>4</sup> Since the imaginary part of the matrix-element product vanishes,<sup>5</sup> the potentially anisotropic term in (3) disappears.

The detector processes referred to do not distinguish between right and left circular polarization or between these and unpolarized radiation. What is needed is a "nuclear quarter-wave plate." One obtains the desired circular polarization detector by using magnetized iron as a Compton scatterer.<sup>6</sup> Then an azimuthal anisotropy in the Compton scattered intensity will arise because the intensities of the right and left circularly polarized components of the radiation are different. In fact, these intensities for unmixed  $2L$ -pole radiation are

$$W(\mathbf{P}_0, \mathbf{k}, P) \sim 1 \pm |P_0| P \frac{J'(J'+1) - L(L+1) - J(J+1)}{L(L+1)(2J_0+1)} \cos \vartheta, \quad (4)$$

where  $(P = \pm 1)$ .

The only essential factor limiting the magnitude of the anisotropy is the relative number of electrons contributing to the magnetization in iron ( $\sim 0.1$ ). As an example of the application of our result we may consider the neutron capture leading to an

even-even compound nucleus and a transition leading to the ground state. Such a transition may be identified by using energy-sensitive detectors. Then, since the anisotropy is determined by the coefficient of  $P$  in (4) a determination of this sign selects one of the two possibilities  $J=J_0 \pm \frac{1}{2}$  and, since  $J=L$ , the sign measurement determines the multipole order of the radiation as well. It should be noted that there are certain exceptional cases where the anisotropy vanishes. The only cases of interest are  $J=2 \rightarrow J'=3$  with the emission of quadrupole radiation ( $L=2$ ) and, considerably less likely,  $J=5 \rightarrow J'=6$  with octupole radiation ( $L=3$ ). Of course,  $J=0$  corresponds to isotropy. So far as dependence on angular momenta is concerned, the anisotropy is maximum when  $J'(J'+1) - J(J+1) = \pm L(L+1)(2J_0+1 \pm 1)$ . This occurs when  $J_0=0$ ,  $J=J'=\frac{1}{2}$  and when  $J_0=\frac{1}{2}$ ,  $J'=0$ ; in both cases  $W \sim 1 \mp |P_0| P \cos \vartheta$  and for these particular cases dipole radiation is expected. Thus, for complete neutron polarization<sup>7</sup> only right, left circular polarization is obtained at  $\vartheta = \pi$ ,  $0$  ( $J=J_0 + \frac{1}{2}$ ) and at  $\vartheta = 0$ ,  $\pi$  ( $J=J_0 - \frac{1}{2}$ ).

A special case of the foregoing considerations was discussed by Halpern.<sup>8</sup>

\* This paper is based on work performed for the AEC at the Oak Ridge National Laboratory.

<sup>1</sup> Biedenharn, Rose, and Arfken, AEC Report, ORNL 986 (March 26, 1951).

<sup>2</sup> G. Goertzel, Phys. Rev. **70**, 897 (1946).

<sup>3</sup> E. U. Condon and G. H. Shortley, *Theory of Atomic Spectra* (Cambridge University Press, London, 1935), Chapter III.

<sup>4</sup> E. P. Wigner, *Gruppen Theorie* (J. W. Edwards, Ann Arbor, Michigan, 1944), reprint. See also reference 3, pp. 76-77.

<sup>5</sup> S. P. Lloyd, Phys. Rev. **81**, 161 (1951). In obtaining (3) the direction of  $\mathbf{P}_0$  was chosen as the axis of quantization. Choosing the latter along  $\mathbf{k}$  we obtain only the first term of (3), which is, of course, isotropic. Since none of the factors in the second term of (3) other than  $\text{Im} [a(JJ'L)a^*(JJ'L')]$  can vanish identically, we obtain an alternative demonstration of Lloyd's result on relative phases of nuclear matrix elements.

<sup>6</sup> See U. Fano, J. Opt. Soc. Am. **39**, 859 (1949), where this result is implicitly contained.

<sup>7</sup> C. G. Shull, Phys. Rev. **81**, 626 (1951).

<sup>8</sup> O. Halpern, Phys. Rev. **82**, 753 (1951).

### Domain Wall Relaxation in Nickel

W. P. MASON

Bell Telephone Laboratories, Murray Hill, New Jersey  
(Received June 11, 1951)

RECENT measurements<sup>1</sup> of the decrement  $\delta$  and the difference between the magnetically saturated and the demagnetized elastic constants (the  $\Delta E$  effect) of nickel have shown that these effects are much smaller at 10 megacycles than they are in the low frequency range. Complete decrement-frequency and  $\Delta E$ -frequency curves have been measured on a well-annealed polycrystalline rod with the results shown by Fig. 1. The decrement has reached a maximum value at about 150,000 cycles, while the  $\Delta E/E_D$  ratio is decreasing continuously with frequency. It is the purpose of this note to show that this effect is due to a relaxation in the domain wall motion caused by the fact that the wall cannot follow the applied stress at high frequencies, on account of the induced micro-eddy-currents.

The simplest model that will demonstrate the  $\Delta E$  effect is the  $90^\circ$  wall model shown by Fig. 2. This model applies to iron, since the directions of easy magnetization lie along cube axes. The equation of motion for such a domain wall for a sinusoidally applied magnetic field  $H$ , is

$$M'(d^2x/dt^2) + R'(dx/dt) + K'x = HI_s e^{i\omega t}, \quad (1)$$

where  $M'$ ,  $R'$ , and  $K'$  are the effective mass, resistance, and stiffness constants of the wall and  $I_s$  is the saturation magnetic intensity. At the low frequencies considered here,  $M'$  can be neglected,  $K'$  can be evaluated from the initial susceptibility, and  $R'$  from power losses.

Taking account of the fact that the domains are distributed in all directions, the average displacement for a field  $H$  is

$$\bar{x} = HI_s / 3K'. \quad (2)$$

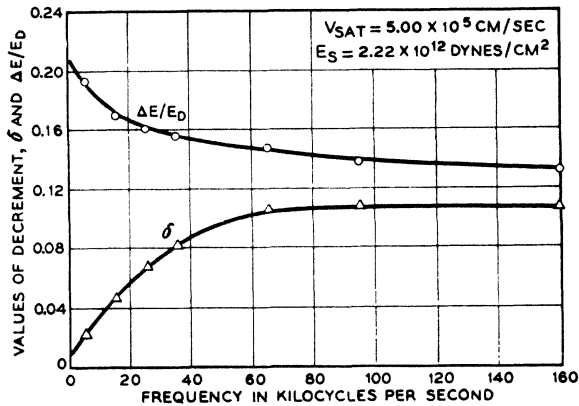


FIG. 1. Values of decrement and  $\Delta E/E_D$  plotted as a function of frequency.

The change in intensity of magnetization associated with the domain wall motion is  $I = \bar{x}I_s/D$ , so that the susceptibility is

$$\chi_0 = I/H = I_s^2/3K'D, \quad \text{or} \quad K' = I_s^2/3\chi_0 D, \quad (3)$$

where  $D$  is the domain thickness in the direction of domain motion.

The power loss for a  $180^\circ$  wall has been calculated<sup>2</sup> by Williams, Shockley, and Kittel for a domain whose cross-sectional area is large compared with its thickness. The loss in a  $90^\circ$  wall will be  $\frac{1}{4}$  of this; and if we equate this power loss to the rate at which the energy is supplied, we have

$$16D^2 I_s^2 v^2 / \pi R = H I_s v D, \quad \text{or} \quad v = \pi R H / 16 D I_s, \quad (4)$$

where  $R$  is the resistivity of the material and  $v$  the velocity of the wall. From Eq. (1), if the dissipative term is controlling, we obtain

$$dx/dt = v = H I_s / R'; \quad \text{hence} \quad R' = 16 D I_s^2 / \pi R. \quad (5)$$

Hence, from Eqs. (1), (2), and (3) the complex susceptibility is

$$\chi = \chi_0 / [1 + jf/f_0],$$

where  $f_0$ , the relaxation frequency, is

$$f_0 = K' / 2\pi R' = R / 96\chi_0 D^2 = \pi R / 24\mu_0 D^2, \quad (6)$$

$\mu_0$  being the initial permeability. This is the same relaxation frequency as that obtained by calculating the eddy current shielding for a plate the same thickness as the domain.

It is difficult to observe this relaxation of the domain wall motion magnetically, since it is obscured by eddy current damping of the whole specimen. However, by using domain wall movements caused by mechanical stresses, no over-all flux is generated and as shown by Fig. 1, this relaxation can be observed. The magnitude

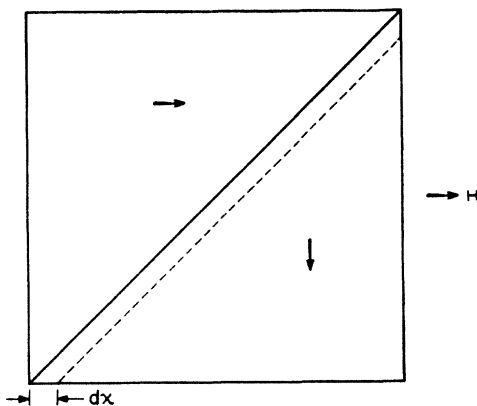


FIG. 2. Domain wall motion for a  $90^\circ$  domain wall.

of the change in the elastic constant ( $\Delta E$ ) and the damping can be calculated by inserting the complex value of the susceptibility in Becker and Döring's expression<sup>3</sup> for the  $\Delta E$  effect. This results in

$$\Delta E/E_D = 9\lambda^2 E_s \mu_0 / 20\pi I_s^2 (1 + jf/f_0) \\ = 9\lambda^2 E_s \mu_0 (1 - jf/f_0) / 20\pi I_s^2 (1 + f^2/f_0^2). \quad (7)$$

The real part of this equation represents the difference between the saturated Young's modulus  $E_s$  and the demagnetized Young's modulus,  $E_D$ , as a function of frequency. The imaginary part represents the dissipation associated with the domain wall motion, and the " $Q$ " of the motion is given by taking the ratio of the real and imaginary parts of the complete elastic constant, i.e.,  $E_s - \Delta E$ . Since the decrement  $\delta$  is  $\pi/Q$ , we have

$$\delta = \frac{9}{20} \left( \frac{\mu_0 \lambda^2 E_s}{I_s^2} \right) \left( \frac{f/f_0}{1 + f^2/f_0^2} \right). \quad (8)$$

The  $90^\circ$  wall model does not represent nickel, which has its easy direction of magnetization along the  $[111]$  directions. Döring,<sup>4</sup> in considering the  $\Delta E/E_D$  effect, has shown that the result of this modification is to replace  $(3/2)\lambda$  by  $\lambda_{111} [5c_{44}/(c_{11} - c_{12} + 3c_{44})]$ , where  $\lambda_{111}$  is the magnetostrictive constant along  $[111]$  direction and  $c_{11}$ ,  $c_{12}$ , and  $c_{44}$  are the three elastic constants of nickel. For  $\lambda_{111} = -25 \times 10^{-6}$ ,  $I_s = 484$ ,  $c_{11} = 2.53 \times 10^{12}$  dynes/cm<sup>2</sup>,  $c_{12} = 1.58 \times 10^{12}$ ,  $c_{44} = 1.23 \times 10^{12}$ , and the measured values of  $\mu_0 = 340$  and  $E_s = 2.22 \times 10^{12}$  dynes/cm<sup>2</sup>, the calculated low frequency value of  $\Delta E/E_D$  is 0.224 and the maximum value of  $\delta$  is 0.353. From the initial slope,  $\delta/f = 2.5 \times 10^{-6}$  and the frequency of maximum decrement  $f_0 = 150,000$  cycles, the average domain size is about 0.05 mm. The actual shape of the  $\Delta E/E_D$  curve of Fig. 1 indicates a distribution of domain sizes from 0.15 mm to 0.02 mm, which is in good agreement with the optical measurements of Williams.<sup>5</sup>

I wish to thank Dr. R. M. Bozorth and Dr. C. Kittel for helpful conversations.

<sup>1</sup> Bozorth, Mason, and McSkimin, Phys. Rev. **83**, 220 (A) (1951). A fuller account is to be published in the October issue of the *Bell System Technical Journal*.

<sup>2</sup> Williams, Shockley, and Kittel, Phys. Rev. **80**, 1090 (1950).

<sup>3</sup> M. Becker and W. Döring, *Ferromagnetismus* (Verlag, Julius Springer, Berlin, 1930), p. 343.

<sup>4</sup> W. Döring, Z. Physik **114**, 579 (1939).

<sup>5</sup> H. J. Williams, to be published.

## Electron Penetration and Scattering in Phosphors

L. R. KOLLER AND E. D. ALDEN  
General Electric Research Laboratory, Schenectady, New York  
(Received May 15, 1951)

THERE is very little experimental data on the loss of energy of electrons in phosphors. The availability in this laboratory of thin uniform chemically deposited layers of phosphors afforded an opportunity of making such measurements. The preparation of these films of zinc sulfide is described in a Letter to the Editor.<sup>1</sup> The films studied were deposited on glass and varied in thickness from about 0.1 to 0.45 micron.

The samples were excited by electron bombardment at voltages from 2 to 40 kv in a demountable post accelerator cathode-ray tube. A film of aluminum  $0.01\mu$  thick was evaporated onto the surface of the phosphor to prevent "sticking." Corrections were made for the energy lost by the electrons in this layer. The brightness at constant beam current (current density  $0.8 \mu\text{a}/\text{cm}^2$ ) as a function of beam voltage was measured with a photomultiplier tube. These quantities were displayed on a cathode-ray oscilloscope and the resulting trace photographed.

A typical voltage brightness relation is shown in Fig. 1. After the initial portion of the curve (not shown here) over which the brightness increases as a power of the voltage, there is a considerable range over which the brightness is a linear function of voltage, after which it passes through a fairly sharp maximum. The point at which the relation deviates from a straight line is interpreted